

# **SUPERSONIC COMBUSTION REGIME: NUMERICAL AND THEORETICAL STUDY**

**A. Ingenito\*, D. Cecere\*\*, E. Giacomazzi\*\***

antonella.ingenito@uniroma1.it

\* Department of Mechanical and Aerospace Engineering, University of Rome La Sapienza,  
via Eudossiana 18, 00184, Rome, Italy

\*\* ENEA Casaccia, UTTEL-COMSO, S.P. 081, Via Anguillarese 301, 00123, S.M. Galeria, Rome, Italy

## **Abstract**

A three dimensional high order numerical simulations of the H<sub>2</sub>/air supersonic combustion were performed. Large Eddies Simulation showed to be a promising tool to investigate the fundamental physical phenomena involved in the flame/turbulence interaction and to support the development of new subgrid scale turbulence and combustion models was investigated using LES simulations. The present LES of the HyShot II supersonic combustor showed that the interactions between the airstream entering the combustor and the H<sub>2</sub> sonic jet produce a high turbulence intensity confirmed by an average vorticity of order 10<sup>5</sup> Hz. The interaction between the hydrogen transverse jets and the supersonic air flow led to the bow shock formation and, accordingly, the boundary layer separation. This separation allowed H<sub>2</sub> to be convected upstream through the spanwise recirculation vortices created by the baroclinic effect. Once created, the vortices were tilted, stretched, compressed and expanded according to the vorticity transport equation. These vortices are the key structures responsible for the observed fast fuel air mixing. In this context, an analysis of the flame structure was conducted to propose a appropriate kinetic and chemical/turbulence model. The flame structure has been analyzed by means of the Burke and Schumann theory.

## **Introduction**

The aim of this work is to investigate the validity of combustion models that were developed for low-speed combustion and then traditionally extended to high-speed combustion. In fact, the assumption of fast chemistry, as well as the flamelet chemistry model, may not be valid in supersonic flows, where compressibility may affect the flame structure. Previous numerical [1] and theoretical results [2] by these authors confirmed that the baroclinic term plays a major role in supersonic mixing and combustion and cannot be neglected, having the same order of magnitude of both vortex stretching and compressibility terms. In fact, the spinning acceleration due to the baroclinic term (locally of order 10<sup>12</sup> ÷ 10<sup>13</sup> rad/s<sup>2</sup>) indicate how strong pressure and density gradients are in the injection region: there, in fact, vorticity increases 10<sup>9</sup> to 10<sup>10</sup> Hz per millisecond.

In fact, crossflow H<sub>2</sub> injection is responsible for the high vorticity production and injection within the flow field: as the sonic hydrogen jet interacts with the

supersonic air crossflow, coherent structures, that contribute to the fuel-air mixing enhancement, develop quickly: there, supersonic and subsonic vortex speeds alternate. LESs show spanwise vortices generated upstream of the H<sub>2</sub> injection are stretched and tilted downstream by vortex stretching. Vortices in between hydrogen jets are also generated by the baroclinic term and are responsible for spreading the fuel over the entire cross section.

The intense vorticity generated in the flow field is responsible for nearly complete combustion: chemical kinetics is very fast, in fact, in about 15 orifice diameters (3 cm downstream of the injectors) the fuel fraction is already down to 50%, and only a very small fraction of H<sub>2</sub> (YH<sub>2</sub>) remains unburnt at the end of the combustor.

The fast kinetic times are confirmed by the presence of water *already upstream* of the fuel injection, suggesting the possibility to implement a one-step kinetic mechanism or a Flamelet-Based model to reduce CPU time due to complex chemical kinetics. In order to select an appropriate flame model in these and similar CFD simulations, analysis of the flame structure and morphology after the hydrogen jets are tilted streamwise is reported in the next section.

### HyShot Combustor Geometry and Simulation Modelling

The HyShot geometry (see Fig. 1, where the computational domain is in blue) consists of a rectangular cross section of 75 x 9.8 mm, 300 mm long. Table 1 reports the inlet conditions of hydrogen and air as injected inside the combustor.

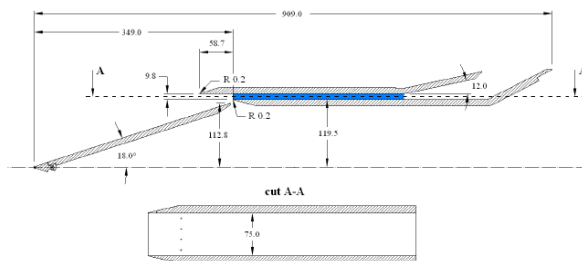


**Figure 1.** Hyshot schematic; portion of the combustion chamber simulated in blue.

**Table 1.** Air/Hydrogen inlet flow condition.

$\phi = 0.426$	Air	Hydrogen
Pressure [Pa]	82110	307340
Mach	2.79	1
Density [kg/m <sup>3</sup> ]	0.2358	0.3020
Temperature [K]	1229	250
Sound speed [m/s]	682.9	1204.4
Flow speed [m/s]	1905.291	1204.4

The structured 3D CFD grid includes about 50 Mnodes (878 streamwise along z and 448 and 128 along x and y, respectively). The cell distribution is refined

around injection holes and near walls. In the spanwise direction, for  $2 \text{ cm} < x < 5 \text{ cm}$ , nodes are more closely spaced to improve the simulation of the pressure gradients due to the interaction of the bow shocks in front of the two central hydrogen jets.

The 3D LES of the HyShot combustor have been performed with the S-HeaRT code. The interface fluxes are evaluated by a hybrid method capable of capturing shocks while at the same time resolving the turbulent structures away from discontinuities with minimal dissipation. This goal was achieved by adopting a 4<sup>th</sup>-order central scheme. In the shock capturing scheme the reconstruction of the Riemann problem at the cell interface is performed by means of a WENO 35 scheme. To obtain the interface fluxes from the reconstructed states the approximate hybrid HLLC/HLLE Riemann solver is implemented [3]. Time-integration is by means of the fully explicit third order accurate TVD Runge-Kutta scheme of Shu and Osher [4]. Partially non-reflecting boundary conditions have been implemented (following the NSCBC technique) to reduce numerical reflection of acoustic waves back into the computational domain [5]. For numerical stability the time step was about  $10^{-9}$  s. The unsteady simulations performed are based on the “eddy viscosity” [FM] SGS Fractal Model [6]. The detailed Warnatz [7] kinetic mechanism involving 9 species and 37 chemical reactions is implemented.

### Numerical Results:Supersonic Flame Structure

In the Hyshot test case, hydrogen and air are separately introduced within the combustor. Thus, as first approximation, the flame can be studied as a turbulent diffusion flame, where the fuel/air ratio are not constant[xii].

In order to evaluate the local structure of the turbulent non premixed/diffusive flames, a Burke and Schumann analysis has been carried out. In particular, flow temperature,  $\text{YH}_2$ ,  $\text{YOH}$ ,  $\text{YO}_2$  and  $\text{YH}_2\text{O}$  as a function of the  $Z$  mixture fraction have been analyzed. The mixture fraction  $Z$  is defined to be 0 in the oxidizer

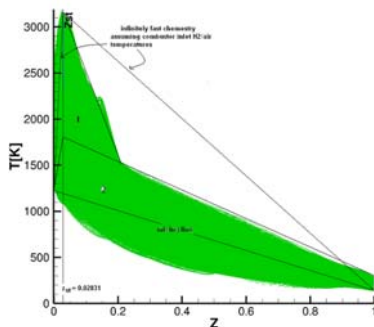
stream, unity in the fuel stream and locally  $z = \frac{1}{\Phi + 1} \left( \Phi \frac{Y_F}{Y_F^0} - \frac{Y_O}{Y_O^0} + 1 \right)$ , where

$$\Phi = s \frac{Y_F^0}{Y_O^0}. \text{ The mixture stoichiometric fraction of } Z \text{ is given by: } z_{st} = \frac{1}{\Phi + 1}.$$

This ratio characterizes the structure of the flames when two streams (fuel and oxidizer) diffuse into each other. For hydrogen/air mixture this value corresponds to  $Z_{st} = 0.02831$  (generally, for these low  $Z_{st}$ , the flame lies close to the oxidizer side while it is located close to the fuel side for large  $Z_{st}$ ). The Burke and Schumann theory [8, 9, 10] states that in a given turbulent diffusion flame all temperature and mass fraction values must be located between the mixing and the equilibrium lines (no other state is possible). Mixing lines are where fuel and oxidizer would mix without reaction. When most points are located close to the mixing line, the flame is

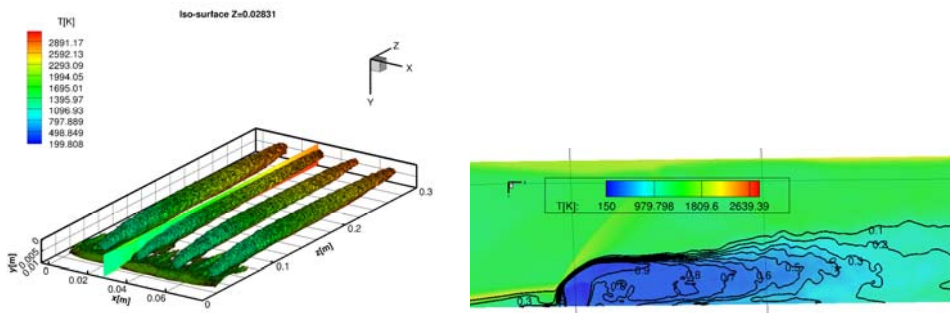
either close to extinction, or not yet ignited. Diagrams where these values are located close to the equilibrium line indicate vigorous flames.

Fig. 2 shows numerical results from the present simulation. A number of points lies below the mixing line: this is due to the fact that the flow is supersonic. In fact, H<sub>2</sub> expansion after injection is responsible for the temperature decreasing, and as a consequence, a number of temperature states are possible, and can thus be found below the mixing line. At the same time, the highest temperatures are reached close to the wall, where the flow decelerates to subsonic speeds and thus raises the static temperature.



**Figure 2.** T versus Z obtained from the present numerical results.

As theoretically predicted, for the low  $Z_{st}$  of the present simulation, the flame is well anchored close to the oxidizer side, i.e., at  $Z < Z_{st}$ .



**Figure 3.** a. Isosurface of  $Z = Z_{st}$  colored by T. b. T field and isolines of Z

At  $Z = Z_{st}$  flow temperatures vary from 1100 K to 3200 K as shown also in Fig. 3a. Fig. 2 shows a number of quenching (or not ignited) points for rich conditions, i.e., for  $Z > Z_{st}$ . This is clearly explained by looking at Fig. 3b, where the temperature and iso-Z lines are shown close to the fuel injection. This figure shows that for  $0.2 < Z < 1$ , the temperatures varies from 150 K to 980 K, i.e., is too low to ignite the locally forming mixture. At  $Z_{st} < Z < 0.2$ , the flow temperatures are higher than 1000K, i.e., the local temperature conditions are large enough to allow flame anchoring: this explains the curve knee corresponding to  $Z = 0.2$ . Accordingly, the

fuel-rich region can be split in two different regions: the first for  $Z_{st} < Z < 0.2$ , corresponding to the part of the combustor from  $z$ -axis = 0.05 m downstream where fuel and oxidizer temperatures are higher than 1000 K; the second region,  $0.2 < Z < 1$ , prevails in the first half of the combustor, where initial temperatures are below 1000 K and ignition conditions are not verified.

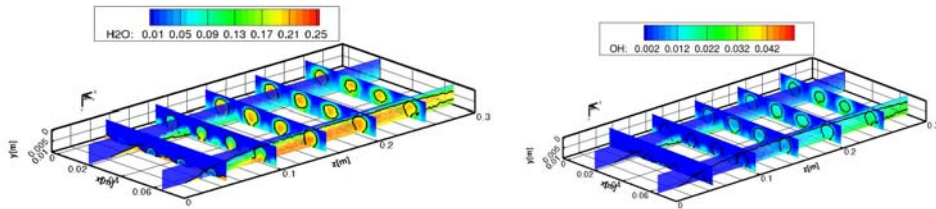


Figure 4. YH<sub>2</sub>O and YO<sub>2</sub>H field and iso-Z<sub>st</sub> lines.

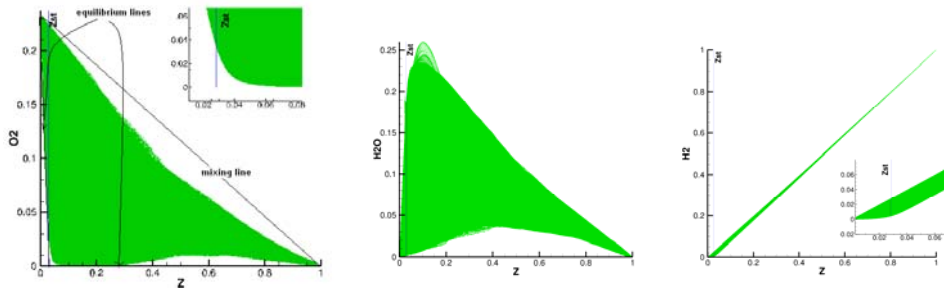


Figure 5. O<sub>2</sub>, H<sub>2</sub>O and O<sub>2</sub> concentrations versus Z.

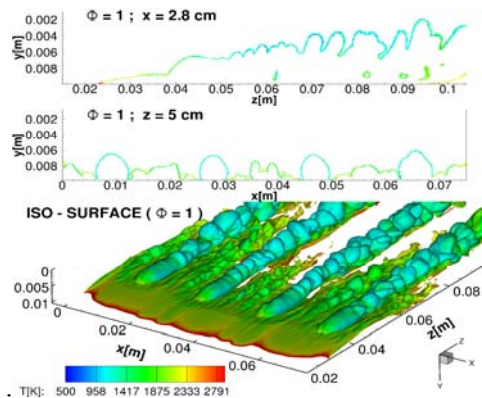


Figure 6. a) Instantaneous stoichiometric flame surface and section views.

This is also supported by Fig. 6 showing a highly corrugated flame for  $z > 50$  mm. The flame length and shape is shown in Fig. 4: it occupies the whole combustor section. Fig. 4 shows a still high OH concentration (about 25%) at the combustor exit, this is due to the dissociation effect caused by the high temperatures. Fig. 5

shows that H<sub>2</sub> and O<sub>2</sub> mass fractions do not follow the *ideal* flame structure, but overlap in the flame region because of *finite rate* chemistry and flame strain rate (stretch). In fact, Fig 5 shows that O<sub>2</sub> differs from the equilibrium lines in the rich region, and that part of the O<sub>2</sub> is not burned. As said, this is the effect of the low temperatures and the short stretching times that quench flame kinetics. In fact, extinction of turbulent hydrogen-air diffusion flame occurs at a strain rate about 14,260 s<sup>-1</sup>, corresponding to a characteristic time 0.64\*10<sup>-5</sup> s. This means that at low temperatures, where kinetics is slower than stretching, the flame is strained and quenched. This of course is not the case where temperatures are high enough and kinetic times are shorter than mixing times.

### Conclusions

The analysis of the supersonic flame structure has shown that the assumption of fast chemistry, as well as flamelet kinetic model may not be an acceptable choice. In fact, a detailed kinetic mechanism capable to account correctly for the kinetic times is required to properly predict flame anchoring and combustion efficiency in a supersonic combustor, where mixing is responsible for a spatial and temporal distribution of fuel and air mixtures varying from  $Z = 0$  to  $Z = 1$ .

### References

- [1] D. Cecere, A. Ingenito, E. Giacomazzi, L. Romagnosi, C. Bruno, "Hydrogen/air supersonic combustion for future hypersonic vehicles", International Journal of Hydrogen Energy, Volume 36, Issue 18, September 2011, Pages 11969-11984;
- [2] A. Ingenito, C. Bruno, "Physics and Regimes of Supersonic Combustion", AIAA J., Vol.48, No. 3, March 2010;
- [3] G.S. Jiang, C.W. Shu, "Efficient Implementation of Weighted ENO Schemes", Division of Applied Mathematics, Brown University, Providence, Rhode Island, 1996;
- [4] C.-W. Shu and S. Osher (1988): Efficient Implementation of essentially non-oscillatory shock-capturing schemes, J. Comput. Phys. 77, 439
- [5] W. Polifke and C. Wall, "Non-reflecting boundary conditions for acoustic transfer matrix estimation with LES", Center for Turbulence Research Proceedings of Summer Program, 2002;
- [6] E. Giacomazzi and C. Bruno and B. Favini, "Fractal Modelling of Turbulent Mixing, Combustion Theory and Modelling", 1999.
- [7] U. Maas and J. Warnatz, "Combustion and Flame", vol. 74, pp. 53-69, 1988.
- [8] Burke, S.P. and Schumann, T.E.W., Ind. Eng. Chem, Vol. 20, N. 998, 1928
- [9] A. Linan, F.A. Williams, Fundamental Aspects of Combustion, Oxford Eng. Science Series 34, 1993
- [10] R. Borghi, M. Destriau, La Combustion et Les Flammes, Technip, 1995